AD-A056 127 AEROSPACE MEDICAL RESEARCH LAB WRIGHT-PATTERSON AFB OHIO F/G 17/7
TERRAIN CONTOUR MATCHING (TERCOM): SENSITIVITY TO HEADING AND G--ETC(U)
MAY 78 M W CANNON

UNCLASSIFIED AMRL-TR-77-84 NL

1 OF 1
AD A056 127

END
DATE FILMED
8-78
DDC

LEVEL II

AMRL-TR-77-84

TERRAIN CONTOUR MATCHING (TERCOM): SENSITIVITY TO HEADING AND GROUND-SPEED ERRORS

MARK W. CANNON, JR.

MAY 1978

Approved for public release; distribution unlimited.

AEROSPACE MEDICAL RESEARCH LABORATORY
AEROSPACE MEDICAL DIVISION
AIR FORCE SYSTEMS COMMAND
WRIGHT-PATTERSON AIR FORCE BASE, OHIO 45433

NOTICES

When US Government drawings, specifications, or other data are used for any purpose other than a definitely related Government procurement operation, the Government thereby incurs no responsibility nor any obligation whatsoever, and the fact that the Government may have formulated, furnished, or in any way supplied the said drawings, specifications, or other data, is not to be regarded by implication or otherwise, as in any manner licensing the holder or any other person or corporation, or conveying any rights or permission to manufacture, use, or sell any patented invention that may in any way be related thereto.

Please do not request copies of this report from Aerospace Medical Research Laboratory. Additional copies may be purchased from:

National Technical Information Service
5285 Port Royal Road
Springfield, Virginia 22161

Federal Government agencies and their contractors registered with Defense Documentation Center should direct requests for copies of this report to:

Defense Documentation Center
Cameron Station
Alexandria, Virginia 22314

TECHNICAL REVIEW AND APPROVAL

AMRL-TR-77-84

This report has been reviewed by the Information Office (OI) and is releasable to the National Technical Information Service (NTIS). At NTIS, it will be available to the general public, including foreign nations.

This technical report has been reviewed and is approved for publication.

FOR THE COMMANDER

WILLIAM J. GANNON
Associate Director
Biodynamics and Bioengineering Division
Aerospace Medical Research Laboratory

AIR FORCE/56780/12 June 1978 — 150

AD56 127

SECURITY CLASSIFICATION OF THIS PAGE *(When Data Entered)*

REPORT DOCUMENTATION PAGE

READ INSTRUCTIONS BEFORE COMPLETING FORM

1. REPORT NUMBER: AMRL-TR-77-84
2. GOVT ACCESSION NO.
3. RECIPIENT'S CATALOG NUMBER

4. TITLE (and Subtitle): TERRAIN CONTOUR MATCHING (TERCOM): SENSITIVITY TO HEADING AND GROUND-SPEED ERRORS
5. TYPE OF REPORT & PERIOD COVERED: Final Report. Mar 1975 - Aug 1977
6. PERFORMING ORG. REPORT NUMBER

7. AUTHOR(s): Mark W. Cannon, Jr
8. CONTRACT OR GRANT NUMBER(s)

9. PERFORMING ORGANIZATION NAME AND ADDRESS: Aerospace Medical Research Laboratory, Aerospace Medical Division, Air Force Systems Command, Wright-Patterson Air Force Base, Ohio 45433
10. PROGRAM ELEMENT, PROJECT, TASK AREA & WORK UNIT NUMBERS: 62202F; 7233-04-16

11. CONTROLLING OFFICE NAME AND ADDRESS: Same as block 9
12. REPORT DATE: May 1978
13. NUMBER OF PAGES: 21

14. MONITORING AGENCY NAME & ADDRESS *(if different from Controlling Office)*
15. SECURITY CLASS. *(of this report)*: UNCLASSIFIED
15a. DECLASSIFICATION/DOWNGRADING SCHEDULE

16. DISTRIBUTION STATEMENT *(of this Report)*

Approved for public release; distribution unlimited

17. DISTRIBUTION STATEMENT *(of the abstract entered in Block 20, if different from Report)*

18. SUPPLEMENTARY NOTES

19. KEY WORDS *(Continue on reverse side if necessary and identify by block number)*

Terrain Contour Matching (TERCOM)
TERCOM Navigation
Pattern Recognition

20. ABSTRACT *(Continue on reverse side if necessary and identify by block number)*

A simulation of the TERCOM navigation system is presented and the effects of a number of error sources are studied. Two error sources are course heading and ground-speed variation. A third source is the fact that the radar altimeter samples the terrain at geographical coordinates lying between coordinates that specify the locations of terrain altitudes stored in the on-board computer. The latter is shown to be an insignificant error with the 400-ft distance between
(Continued on reverse)

DD FORM 1 JAN 73 1473 EDITION OF 1 NOV 65 IS OBSOLETE

SECURITY CLASSIFICATION OF THIS PAGE *(When Data Entered)*

DDC 850

20. ABSTRACT (cont)

sample points. Course heading and ground-speed errors are shown to be critical problems when they occur simultaneously. Maximum acceptable errors are approximately two degrees course heading at ±3% expected ground speed.

+ or - 3%

1473 B

783 804

PREFACE

The work discussed in this report was performed under Work Unit 72330416, Self-Organizing Control/RPV Augmentation. This work supplements AMRL Technical Report AMRL-TR-73-130, TERCOM Performance: Analysis and Simulation, by presenting the effect of two common errors, heading and ground speed, on the TERCOM model derived in that report. Improvements of terrain generation have also been incorporated so that realistic non-Gaussian terrain may be treated. The analysis and simulation work was performed in the Mathematics and Analysis Branch of the Biodynamics and Bioengineering Division, Aerospace Medical Research Laboratory during the period March 1975 to August 1977.

INTRODUCTION

The terrain contour matching (TERCOM) navigation system is proposed as an automatic updating device to be used as a supplement to standard inertial navigation systems. The aircraft using TERCOM samples the terrain amplitudes beneath its flight path by means of a radar altimeter and stores a string of N samples in a temporary on-board computer memory. This vector, composed of the N-terrain samples, is then compared with all N-component amplitude vectors extracted from an amplitude array in permanent memory, representing the topography of the terrain over which the aircraft is expected to be flying. The best match between sampled and stored vector determines the ground track over which the aircraft has just flown and hence its geographical position. This system requires that the inertial system be accurate enough to place the aircraft inside the boundaries of the terrain map stored permanently in the on-board computer. A typical mission would consist of a number of inertial legs with a TERCOM position check at the end of each to assure more accurate navigation than could be achieved with the inertial system alone. The algorithms proposed for use in matching the stored terrain vector with the sampled terrain vector are the MAD (minimum average distance) classifier and the MSD (minimum mean squared distance) classifier. The MAD classifier, which is preferred because of its computational simplicity, was studied in a previous report (ref 1) and was shown to give essentially the same performance as the MSD classifier under all conditions studied under ref 1.

TERRAIN SAMPLING ERRORS

In the previous report (ref 1) the terrain amplitude sampled by the aircraft was assumed to have had the same geographical coordinates as some subset of the terrain amplitudes stored in the on-board computer memory. Such a condition is shown in Figure 1, in which a sample terrain section is shown. The h axis designates the terrain amplitude above (or below) some reference plane. The amplitudes representing this terrain that are stored in the on-board computer are denoted by the length of the vertical line between the reference plane and the heavy dots at the intersections of the X and Y grid lines. The row of crosses running across the middle of the terrain represent the location of the amplitudes sampled by the aircraft as it flies over the real terrain. Gaussian noise was added to the stored terrain to account for aircraft sampling errors, errors in stored terrain altitude values and all other possible errors. This was certainly an oversimplification, since all noise sources were assumed additive at all levels. This assumption is not true for a combination of heading and ground-speed errors, as shown later in the report.

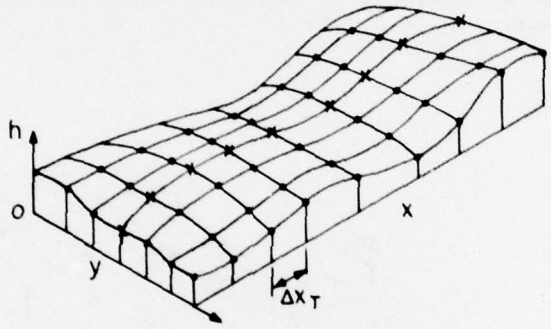

Figure 1. Terrain sample showing stored amplitudes and sampled amplitudes for original TERCOM analysis.

A more realistic approximation is shown in Figure 2, where the aircraft sampling of altitudes may occur anywhere on the x, y plane. Figure 2 shows a possible sampling track in which the distance between aircraft sample points (ΔR_A) is still equal to the distance between the sample points stored in memory (ΔX_T) and the track runs parallel to the axis. Figure 3 shows a condition where aircraft ground speed is slightly faster than the programmed speed, so the distance between aircraft sample points (ΔR_A) is greater than ΔX_T. If ground speed were lower than the programmed speed, ΔR_A would be less than ΔX_T. Figure 4 shows an example of a course heading error σ. The track is no longer parallel to the X axis, but $\Delta R_A = \Delta X_T$, so the ground speed is correct. A final condition where both ΔR_A and σ vary was studied so that the interaction between the two could be investigated.

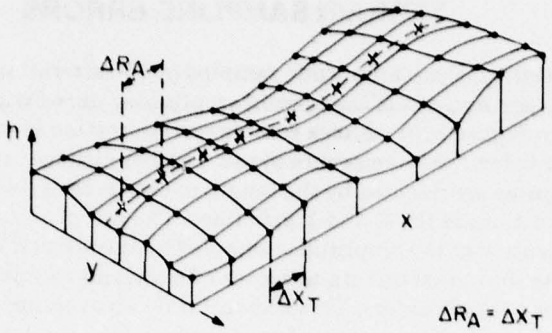

Figure 2. Terrain sample showing stored amplitudes and sampled amplitudes with no groundspeed or heading error.

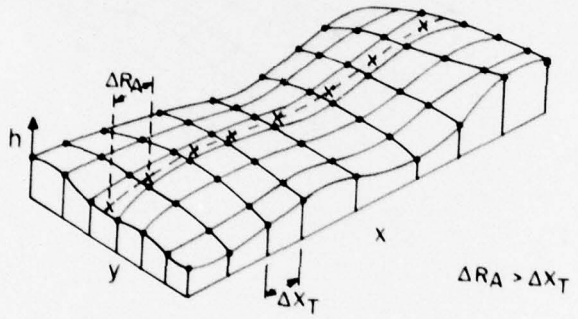

Figure 3. Terrain sample showing stored amplitudes and sampled amplitudes with a groundspeed error but no heading error.

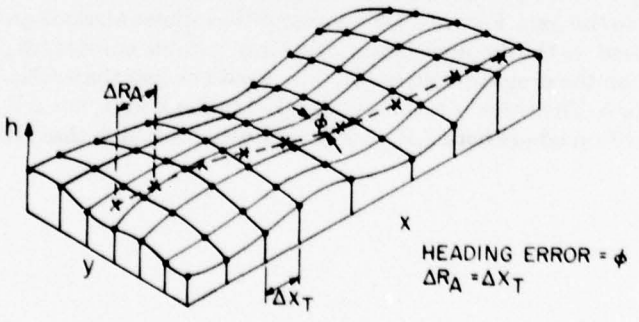

Figure 4. Terrain sample showing stored amplitudes and sampled amplitudes with a heading error.

TERRAIN GENERATION

Experience with terrain generation gained in previous work showed that typical real terrain arrays contain both flat and hilly areas (ref 1). Amplitude histograms computed from a large area of real terrain appeared to be nearly Gaussian. However, amplitude histograms computed from smaller areas of this same terrain array were non-Gaussian. (The distance between sample points on these arrays was 400 ft.) The non-Gaussian behavior of the smaller terrain samples and visual inspection of these same samples indicated that more realistic terrain could be generated from a non-stationary amplitude distribution. The comparison of simulation runs for real and artificially generated terrain in ref 1 showed that TERCOM performance over artificial terrain was the same as for real terrain if a certain parameter ratio, σ_Z/σ_T, was the same for both types of terrain. The parameter σ_Z is defined as $\sigma_Z^2 = E\{(X_i - X_{i+1})^2\}$ where E denotes expectation and the X_i are the terrain sample points. σ_T is just the variance of the sample amplitudes. σ_Z gives a measure of terrain roughness, but it was found that σ_Z/σ_T was more informative than σ_Z alone. A small σ_Z/σ_T indicates smooth terrain with little variation between the sampled amplitudes, but possible large, slow fluctuations in amplitude over the entire area. A large (σ_Z/σ_T) indicates large variation between adjacent sample points but possible small variation in overall amplitude. It was found that σ_Z/σ_T values in the range required could not be produced by artificial terrain generated by a stationary Gaussian process. The first method used to introduce nonstationarity was simply to generate a Gaussian distribution of terrain amplitudes and then to set all amplitudes in a number of adjacent rows of the array equal to zero to produce flat areas. The number of rows set equal to zero was adjusted until the value of σ_Z/σ_T matched that of a particular set of real terrain amplitudes. A different approach was clearly required to remove the amplitude discontinuities present in this procedure. The algorithm finally derived involves the generation of a Gaussian, correlated-amplitude array from the method developed by Moshman (ref 3) and described in Appendix B of ref 1, and the multiplication of this array by a gain function that varies with distance in one direction across the array.

The gain function is

$$G(X) = \frac{1}{(1 + X/X_0)^2}$$

where X_0 is the X coordinate of the center point of the array.

In terms of terrain sample points, X_i, where $i = 1, 64$,

$$G(X_i) = \frac{1}{[1 + (X_i - 1)/X_0]^2} \qquad \text{where } X_0 = 32.$$

The value of σ_Z/σ_T is adjusted by changing X_0, the coordinate where $G(X_i) = .25$.

This is the form of G(X) used by the computer program in appendix A. A typical terrain array generated by this program is shown in Figure 5. An amplitude histogram of this array, shown in Figure 6, displays a non-Gaussian shape. However, ten arrays were generated, and when all were normalized to have the same mean amplitude of zero, the histogram resulting from the combination of all ten is essentially Gaussian, as shown in Figure 7.

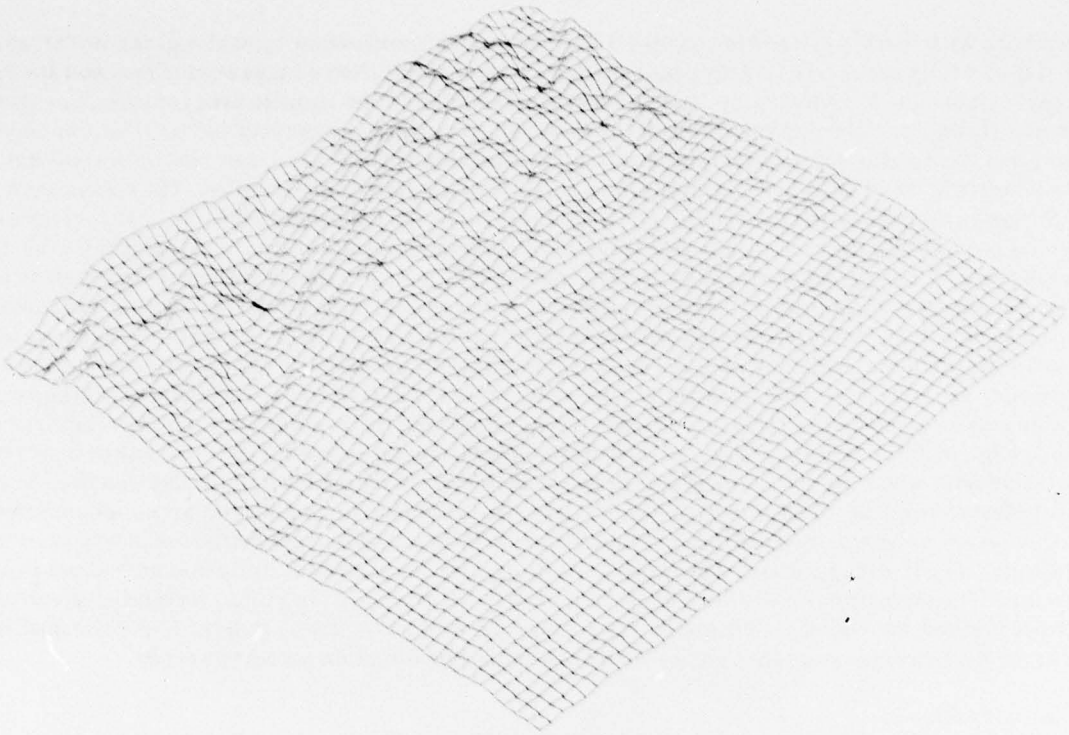

Figure 5. Typical terrain array.

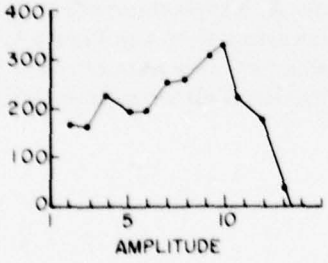

Figure 6. Amplitude histogram of terrain in Figure 5.

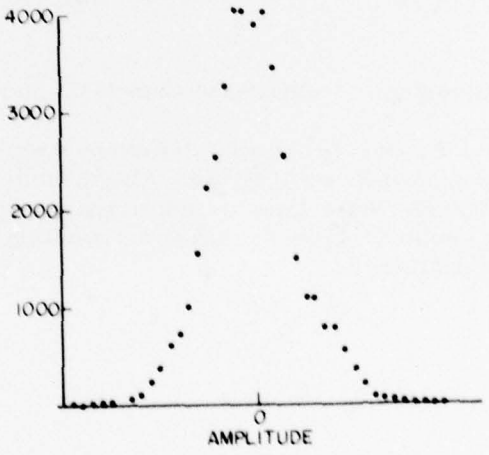

Figure 7. Amplitude histogram of all 10 terrains combined.

FLIGHT SIMULATION PROGRAM

This program was separate from the terrain generation program and used ten pre-prepared terrain arrays to simulate TERCOM runs with variations in ground speed and course heading. The program read in a particular 64x64 terrain array and set up two representations of the array in computer memory. One representation (array S) was served as the array stored in the aircraft's on-board memory. Noise of a selected level was added to this array, point by point, to simulate errors introduced in transcribing terrain amplitudes from small scale aerial photographs or maps (ref 2). This noise may be correlated or uncorrelated; both types were tested.

The second representation (array R) was used to simulate the actual terrain over which the aircraft was flying. The radar altimeter values were obtained from this array. The track length of each TERCOM run was 48 points out of the available 64. Following the information in ref 2, the distance between points was set equal to 400 ft. Each such distance will be referred to as a cell length. This makes the average 48-cell track length equal to 19,200 ft or about 3.6 miles. Track starting coordinates were chosen at random but limited to assure that the entire 48-point track would lie within the 64x64 array.

The runs proceeded in a direction parallel to the X axis. It was assumed that terrain sampling noise in the radar altimeter samples from array R would be much smaller than errors present in the on-board computer representation; array S (ref 2). Therefore, no noise was added to the track obtained from array R.

As mentioned earlier, this simulation allows the track to begin at any X and Y coordinate (that would allow the track to be completely within the array) and not just at the discrete points represented in the on-board terrain array. Both terrain arrays represented in the flight simulation program exist only as discrete amplitudes at coordinates x_i and y_i, which I will call I and J, respectively. The method used to extrapolate the terrain between the I and J coordinates in array R, for use as the radar altimeter sampled values, is very simple. The three sets of (I, J) coordinate pairs nearest to each (X, Y) coordinate pair are determined by the program, and a plane is defined by the three sets of terrain amplitudes A(I, J). The terrain amplitude at (X, Y) called H(X, Y) is then defined as the distance between this plane and the H = O plane. An illustration of this linear interpolation method is shown in Figure 8. In a typical track generated by the program, none of the X,Y coordinate pairs coincide with an I,J coordinate pair.

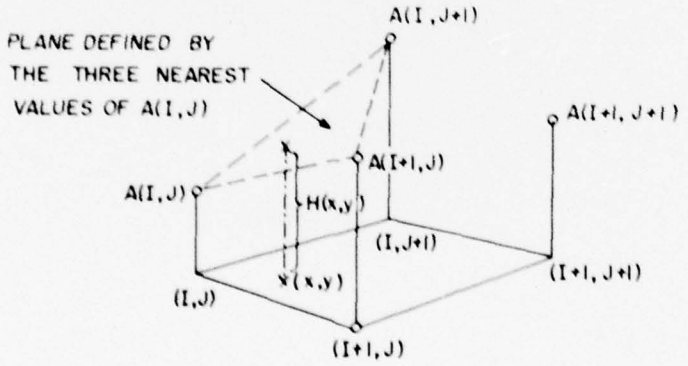

Figure 8. Terrain amplitude extrapolation method.

To simulate ground-speed errors, a parameter ratio V/V_0 was entered into the program. V was the true ground speed while V_0 was the programmed or expected ground speed at which $\Delta R/\Delta X_T = 1$. The maximum V/V_0 ratio used was 1.1 and the minimum was .9, representing about a $\pm$ 10% change in ground speed. This produced a maximum track length of 48 x 1.1 = 52.8 cells. This lengthening of the sampled track constrained the x coordinates of the randomly selected starting points to $X < 11$ in order that the entire 48-point track should fit within the array.

The final effect was the introduction of course heading errors. The maximum angular error considered was 8°. This further limited the random starting coordinates along the y axis. If the maximum possible track length was 53 cells and the maximum angle was 8°, the projection of this track on the y axis was 53 sin 8°, which is about 7.4 cells. The y axis starting coordinates were thus limited to the region $8 < y < 56$.

SIMULATION RESULTS

TERCOM PERFORMANCE WITH SYSTEM NOISE ONLY

The terrain generation and track placement methods were changed sufficiently between this report and the previous one (ref 1) that it is worthwhile to compare some results from ref 1 to the new data. Most of the performance results in the previous report were plotted in terms of the number of correct position fixes vs. σ_Z/σ_N (σ_N is the standard derivation of the additive noise). Since none of the tracks in the present simulation fall on the exact I and J coordinates of the stored terrain, a correct position identification will be defined as a fix (in terms of I and J) within one cell length of the track starting coordinates. The values of σ_Z/σ_T for the ten terrains generated range from .1 to .33, so the results were compared to a performance curve from ref 1 which had been computed on terrain with a σ_Z/σ_T of .2. This comparison is shown in Figure 9 for the case when noise added to the terrain was uncorrelated. The solid curve represents the data of ref 1 and the points represent the new data. Each point represents the average of ten runs on a particular terrain array at the level of σ_Z/σ_N indicated. Clearly there is almost no change between new and old data. Starting the track at points between the I,J geographical coordinates has no effect as long as the ground speed and course heading are the programmed values. Another method of looking at the data is shown in Figure 10 where the average miss distance is plotted as a function of σ_Z/σ_N.

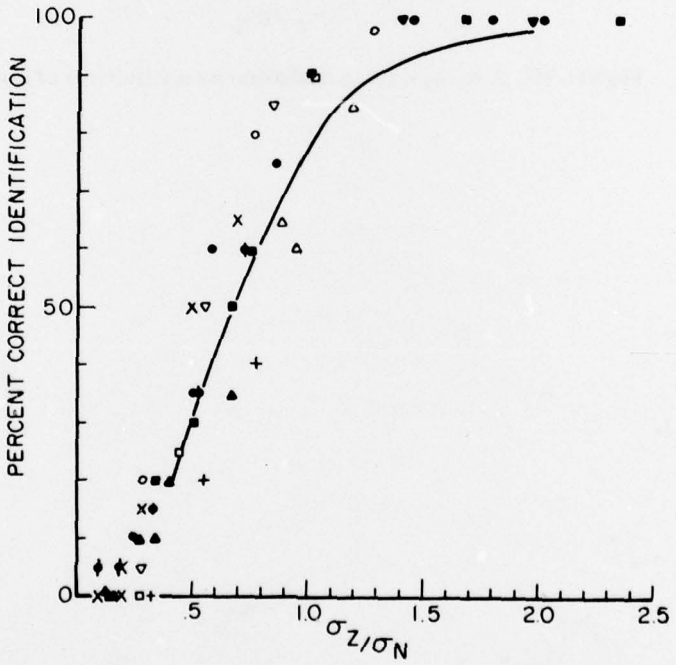

Figure 9. Percent correct responses (within 1 cell of correct location) for $\tau_N = 0$ and $\tau_T = 1024$ cells.

It is evident that for low σ_Z/σ_N values (high noise levels) the error in location can be as large as 6000 to 8000 ft. However, for values of σ_Z/σ_N greater than 1.5 we have an almost perfect correct fix score. A similar plot is shown in Figure 11, where the noise added to the terrain is correlated and has the same correlation length as the terrain. In this case, the miss distance does not descend as rapidly as it does in Figure 10, and perfect fix capability is not reached until $\sigma_Z/\sigma_N > 2.5$. The average miss distances at lower σ_Z/σ_N values are also higher than those shown in Figure 10.

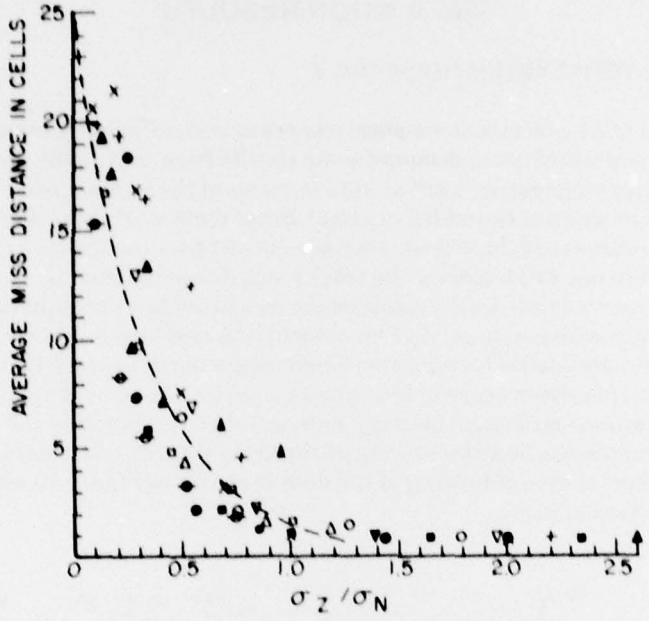

Figure 10. Average miss distance as a function of σ_Z/σ_N.

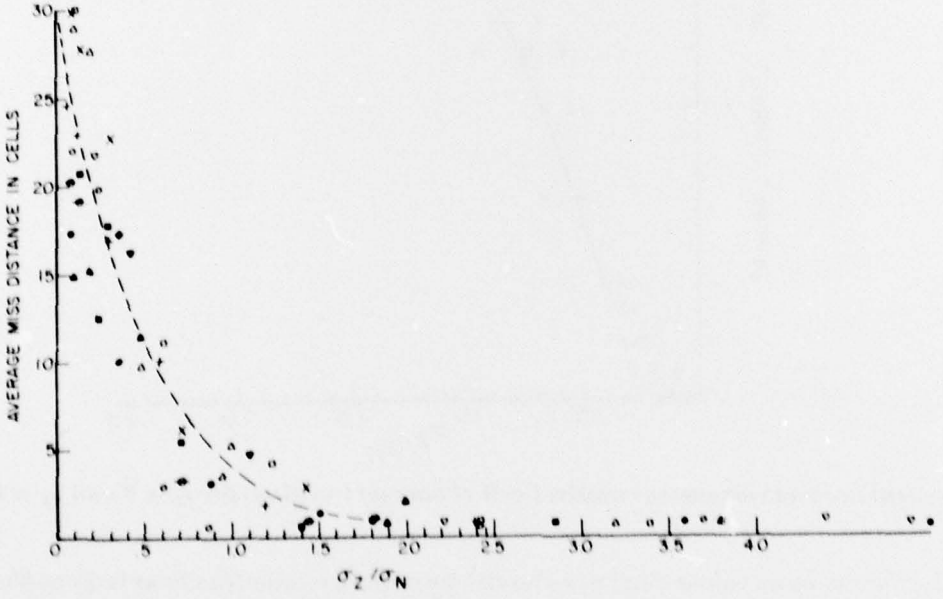

Figure 11. Average miss distance with correlated noise (noise correlation length = 1024 cells).

TERCOM PERFORMANCE WITH VARIATION IN GROUND SPEED AND COURSE HEADING

The effect of ground speed variation was carried out under conditions where σ_T/σ_N was greater than 100, and σ_Z/σ_N was greater than 10, thereby minimizing noise effects from sources other than ground-speed variation. This simulation assumes that the aircraft is sampling terrain amplitudes at a fixed rate so that variations in ground speed about V_0 will cause the geographical distance between sample points to vary about the expected 400-ft intervals. The effect of a constant ground-speed error is shown in Figure 12 where an asymmetry in performance is evident about the value $V/V_0 = 1$. It is seen in Figure 12 that the average and the variance of the miss distance grow more rapidly for $V/V_0 < 1$ than for $V/V_0 > 1$ – an unexpected result. Figure 13 shows the increase in average miss distance as the course heading error increases from 0° to 8°. Again, each point represents 10 trials on a particular terrain, and the mean is computed from 100 trials distributed over 10 terrains. Here, σ_Z/σ_N is greater than 2; large enough to ensure an average miss distance under 1 cell length for 0° heading error.

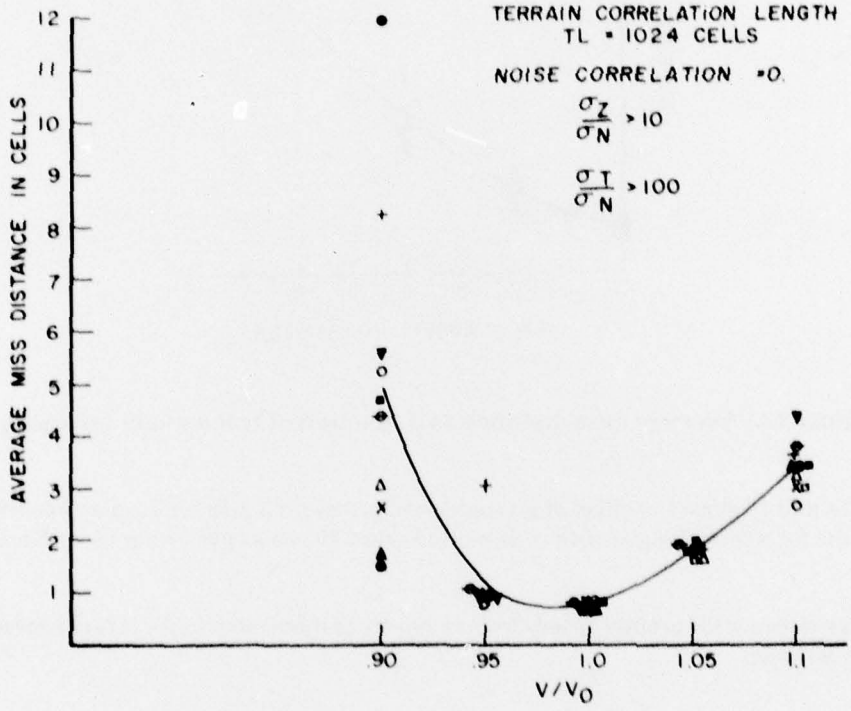

Figure 12. Variation in average miss distance with aircraft speed for no heading error.

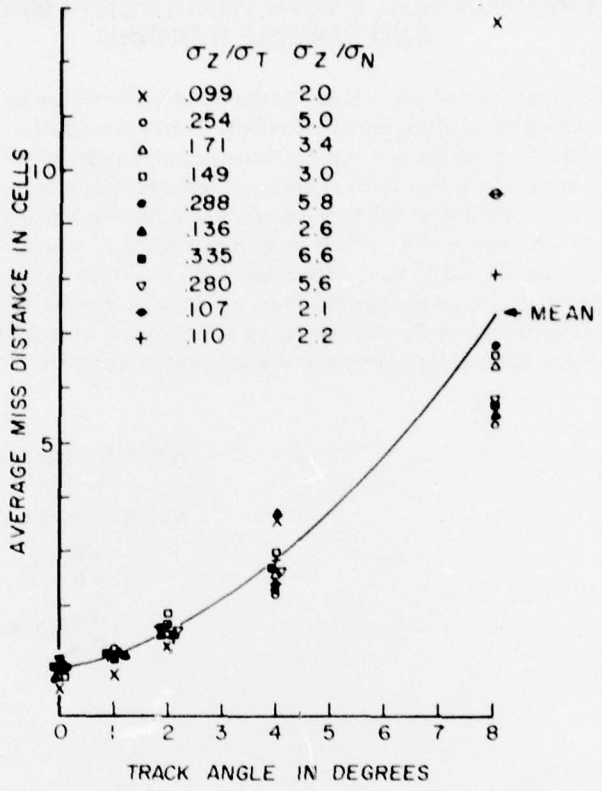

Figure 13. Average miss distance as a function of track angle for $\sigma_Z/\sigma_N > 2$.

Finally, Figures 14 and 15 show the effect of ground-speed errors for 3 different course heading errors. Figure 14 shows the results for a track length of 48 cells while Figure 15 shows performance with a shorter track length of 32 cells.

The increased miss distance for ground speeds lower than V_0 is more evident for larger course heading errors and smaller track lengths.

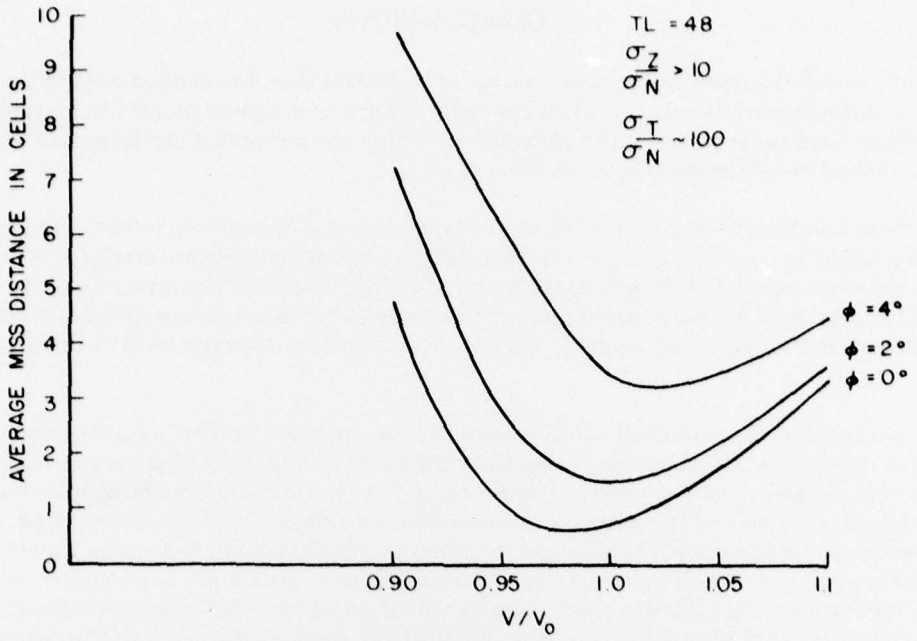

Figure 14. TERCOM performance as a function of groundspeed error with heading error as a parameter.

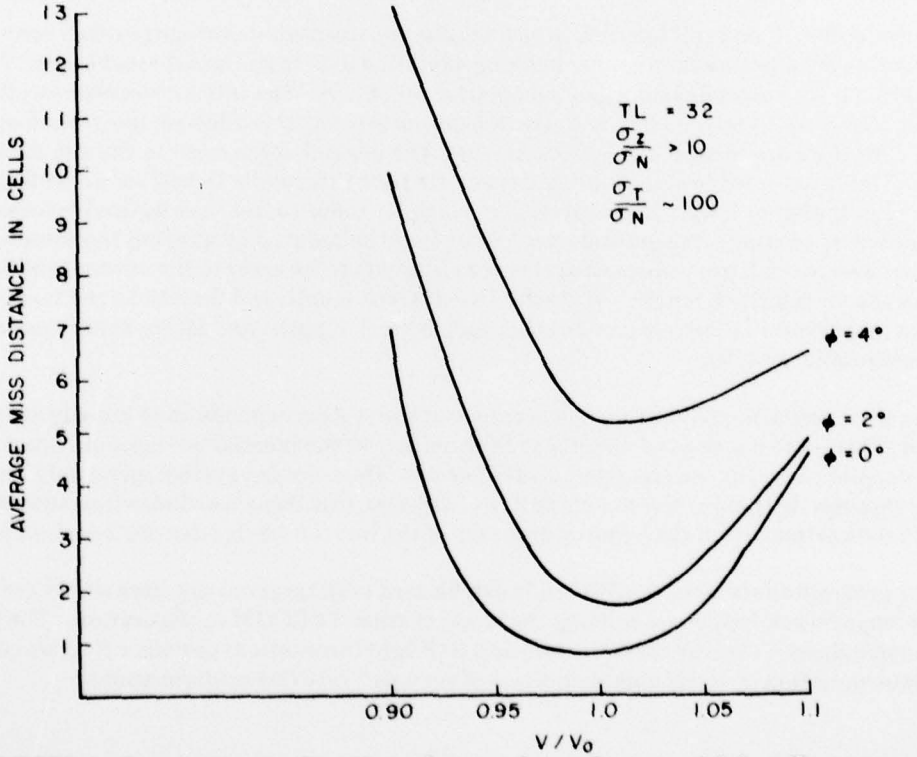

Figure 15. TERCOM performance as a function of groundspeed error with heading error as a parameter.

CONCLUSIONS

This simulation provided a more realistic simulation of TERCOM than the method used in the previous report (ref 1). The simulation showed that even when the radar altimeter sampling points fell between the X and Y coordinates of the amplitudes stored in the on-board computer, the per cent of positions identified correctly remained about the same function of σ_Z/σ_N as those of ref 1.

Apparently, there is sufficient correlation between sample points in the terrain model so that correct fixes can be made with probability $> .95$ for $\sigma_Z/\sigma_N \geq 1.5$ if the additive system noise is uncorrelated. With correlated noise having the same correlation length as the terrain, we saw that the 95% correct fix range is $\sigma_Z/\sigma_N > 2.0$. This result is in agreement with the findings of ref 2 that correlated noise causes a higher error rate than uncorrelated noise. For longer track lengths, it is expected that the σ_Z/σ_N ratio for 95% correct fixes would be lower.

TERCOM may be used with unmanned vehicles such as long-range RPVs. Performance of precision attack or reconnaissance missions will require remote operator intervention during the target approach phase of the flight. Present control philosophy envisions a video feedback to the operator, enabling him to identify the target or specific landmarks and to make course corrections or weapons launches as required. However, due to the enemy electronic detection and the subsequent jamming threat, it is felt that video transmission time should be held to a minimum, and consequently video frame rates may be less than normal. All this implies that the RPV operator should find his vehicle close to the target when video transmission begins, or he may not be able to locate it at all. Studies underway at AMRL/BBM indicate that even with a narrow field of view, say 20°, and an altitude between 500 to 1000 ft, a positioning error of around 1000 ft still gives the RPV operator enough time to maneuver the vehicle over the target or to release weapons.

If we then consider 800 ft, or 2 cell lengths, to be a maximum acceptable average position error, we see from Figure 14 that this error occurs for a course heading deviation of 2° from the expected course. Figure 11 shows that this criterion is also exceeded for a ground-speed error of ±5%. The interaction between these two error sources shown in Figure 14 tells us that if a course heading error of 2° is allowed, the ground-speed error must be limited to ±3% if we are to meet our 800 ft criterion. The ground-speed error in the simulation occurs because TERCOM is assumed to sample altitudes at a fix time rate, while the actual aircraft ground speed may be somewhat higher or lower than expected. If a doppler radar system can be used to measure ground speed with sufficient accuracy, the ground-speed error could be reduced by altering the sampling rate of TERCOM. However, even if ground-speed errors are eliminated, the error in the course heading must be kept to below 2° for the 48-cell track length. While the 48-cell track length and the 64x64-cell terrain matrix are reasonable for an operational system (ref 2), other longer track lengths and larger array sizes may be preferred for greater positioning accuracy.

Nevertheless, the calculations show that the accuracy of the system depends most heavily on the course heading error. This in turn is related directly to the accuracy of the inertial navigation system, and cannot be corrected by doppler radar, as can the ground-speed errors. Thus, for any system using only inertial and TERCOM navigation (with no external aids such as LORAN), this study concludes that successful use of TERCOM depends primarily on the heading accuracy of the inertial navigation system chosen for the aircraft.

The computer programs developed for this study can be used with larger array sizes which are not necessarily square and a longer track length, permitting the study of other TERCOM configurations. The programs which are listed in appendices A (Terrain Generation) and B (Flight Simulation) provide a flexible computational tool for the determination of acceptable accuracies of various TERCOM configurations.

APPENDIX A
TERRAIN GENERATION PROGRAM

```
      PROGRAM TER2(INPUT,OUTPUT,TAPE1)
      DIMENSION A(64,64)
      ID=1
      IDIM=64
      FMEAN=0.
      E=5.
      CALL RANSET(E)
      SIGNO=20.
      TC=1024.
      NEX=2
      XO=40.
      DO 100 NCTR=1,10
      DO 20 I=1,IDIM
      DO 20 J=1,IDIM
      A(I,J)=0.
   20 CONTINUE
      IF(TC.NE.0.)GO TO 24
      RO=0.
      RO1=0.
      GO TO 25
   24 RO=EXP(-1./TC)
      RO1=EXP(-SQRT(2.)/TC)
   25 ACA=RO/(1.+RO1)
      ACB=SQRT(1.-2.*((RO)**2)/(RO1+1.))
      CALL RAND2(RN1,RN2,SIGNO,FMEAN,ID)
      RN3=RN2
      DO 30 I=1,IDIM,2
      CALL RAND2(RN1,RN2,SIGNO,FMEAN,ID)
      A(I,1)=RO*RN3+SQRT(1.-RO**2)*RN1
      A(I+1,1)=RO*A(I,1)+SQRT(1.-RO**2)*RN2
      RN3=A(I+1,1)
   30 CONTINUE
      DO 31 J=2,IDIM
      CALL RAND2(RN1,RN2,SIGNO,FMEAN,ID)
      A(1,J)=RO*A(1,J-1)+SQRT(1.-RO**2)*RN1
      A(2,J)=ACA*(A(1,J)+A(2,J-1))+ACB*RN2
      DO 31 I=3,IDIM,2
      CALL RAND2(RN1,RN2,SIGNO,FMEAN,ID)
      A(I,J)=ACA*(A(I-1,J)+A(I,J-1))+ACB*RN1
      A(I+1,J)=ACA*(A(I,J)+A(I+1,J-1))+ACB*RN2
   31 CONTINUE
      DO 35 I=1,IDIM
      DO 35 J=1,IDIM
      A(I,J)=A(I,J)*(1./(1.+(FLOAT(J-1)/XO)**NEX))
   35 CONTINUE
      WRITE(1) NCTR,((A(I,J),I=1,IDIM),J=1,IDIM)
  100 CONTINUE
      PRINT 102,NCTR,E
  102 FORMAT(10X,*NCTR=*I2,5X,*E=*E15.7)
      CALL RANGET(P)
      PRINT 103,P
  103 FORMAT(10X,*P=*E15.7)
      REWIND 1
      STOP
      END
```

APPENDIX B
TERCOM FLIGHT SIMULATION PROGRAM

```
      PROGRAM TER (INPUT,OUTPUT,TAPE1)
      DIMENSION A(64,64),S(64),A3(64,64)
      DIMENSION RN(64)
      RO=.9990239
 5    E=.7642672
      PNN=1.05
      NL=48
      NBL=64
      NL5=NBL-NL
10    BL5=FLOAT(NL5)
      BL5=11.
      CALL RANSET(E)
      PRINT 107,E
      PRINT 101
15    ANUM=SNUM=DMSD=DMAD=0.
      DO 72 NC=1,10
      AD1=SD1=AD2=SD2=0.
      READ(1) NCTR,A
      PRINT 104,NC
20    SUM10=0.
      SUM11=0.
      RA=20.
      PHI=0.
      PRINT 102,PHI
25    PHI=(PHI/180.)*3.1415926
      FMEAN=0.
      IK=JK=64
      BN=FLOAT(IK*JK)
      SUM=0.
30    BN2=FLOAT(IK-1)
      DO 10 I=1,IK
      DO 10 J=1,JK
      SUM=SUM+A(I,J)
   10 CONTINUE
35    AVE=SUM/BN
      SUM=0.
      DO 20 J=1,JK
      DO 20 I=1,IK
      SUM=SUM+(A(I,J)-AVE)**2
40 20 CONTINUE
      SIGT=SQRT(SUM/BN)
      SIGNO=SIGT/RA
      ID=1
      IF(RO.NE.0.)GO TO 22
45    RO1=0.
      GO TO 25
   22 IF(RO.NE.1.)GO TO 23
      RO1=1.
      GO TO 25
50 23 SCN=-1./ALOG(RO)
      RO1=EXP(-SQRT(2.)/SCN)
   25 ACA=RO/(1.+RO1)
      ACB=SQRT(1.-2.*((RO)**2)/(RO1+1.))
      CALL RAND2(RN1,RN2,SIGNO,FMEAN,ID)
55    RN3=RN2
      DO 30 I=1,64,2
      CALL RAND2(RN1,RN2,SIGNO,FMEAN,ID)
```

```
      RN(I)=R0*RN3+SQRT(1.-R0**2)*RN1
      RN(I+1)=R0*RN(I)+SQRT(1.-R0**2)*RN2
   60 SUM10=RN(I)**2+RN(I+1)**2+SUM10
      SUM11=RN(I)+RN(I+1)+SUM11
      AB(I,1)=A(I,1)+RN(I)
      AB(I+1,1)=A(I+1,1)+RN(I+1)
      RN3=RN(I+1)
   65 30 CONTINUE
      DO 31 J=2,64
      CALL RAND2(RN1,RN2,SIGNO,FMEAN,ID)
      RN(1)=R0*RN(1)+SQRT(1.-R0**2)*RN1
      RN(2)=ACA*(RN(1)+RN(2))+ACB*RN2
   70 SUM10=RN(1)**2+RN(2)**2+SUM10
      SUM11=RN(1)+RN(2)+SUM11
      AB(1,J)=A(1,J)+RN(1)
      AB(2,J)=A(2,J)+RN(2)
      DO 31 I=3,64,2
   75 CALL RAND2(RN1,RN2,SIGNO,FMEAN,ID)
      RN(I)=ACA*(RN(I-1)+RN(I))+ACB*RN1
      RN(I+1)=ACA*(RN(I)+RN(I+1))+ACB*RN2
      SUM10=RN(I)**2+RN(I+1)**2+SUM10
      SUM11=RN(I)+RN(I+1)+SUM11
   80 AB(I,J)=A(I,J)+RN(I)
      AB(I+1,J)=A(I+1,J)+RN(I+1)
   31 CONTINUE
      SUM=0.
      DO 52 J=1,JK
   85 DO 52 I=1,IK
      SUM=SUM+AB(I,J)
   52 CONTINUE
      SUM=SUM/4096.
      DO 53 J=1,JK
   90 DO 53 I=1,IK
      AB(I,J)=AB(I,J)-SUM
   53 CONTINUE
      SDEVN=SQRT(SUM10/4096.-(SUM11/4096.)**2)
      IF(SDEVN.NE.0.)GO TO 40
   95 SNR=11.11
      GO TO 41
   40 SNR=SIGT/SDEVN
   41 PRINT113,SDEVN,SIGT,SNR
      ID=2
  100 DO 70 L=1,10
      CALL RAND2(RN1,RN2,SIGNO,FMEAN,ID)
      YO=(8L5*RN1)+1.
      XO=(45.*RN2)+10.
      KI1=YO
  105 KJ1=XO
      PN=0.
      DO 42 M=1,NL
      X=PN*SIN(PHI)+XO
      Y=PN*COS(PHI)+YO
  110 I=IFIX(Y)
      J=IFIX(X)
      P=(Y-FLOAT(I))/(X-FLOAT(J))
      IF(P.GE.1.)GO TO 43
      G1=(A(I,J)-A(I,J+1))*(FLOAT(J+1)-X)
```

```
115               B2=(A(I+1,J+1)-A(I,J+1))*(Y-FLOAT(I))
                  S(M)=B1+B2+A(I,J+1)
                  GO TO 44
                43 B1=(A(I,J)-A(I+1,J))*(FLOAT(I+1)-Y)
                  B2=(A(I+1,J+1)-A(I+1,J))*(X-FLOAT(J))
120               S(M)=B1+B2+A(I+1,J)
                44 PN=PN+PNN
                42 CONTINUE
                  SUM=0.
                  DO 55 I=1,NL
125               SUM=SUM+S(I)
                55 CONTINUE
                  SUM=SUM/NL
                  DO 56 I=1,NL
                  S(I)=S(I)-SUM
130             56 CONTINUE
                  NL2=64-NL+1
                  SUMR=32000.
                  SUMR2=1.E7
                  DO 62 J=1,JK
135               DO 62 K=1,NL2
                  SUM=0.
                  SUM2=0.
                  SUM5=0.
                  DO 58 I=1,NL
140               II=I+K-1
                  SUM5=AB(II,J)+SUM5
                58 CONTINUE
                  SUM5=SUM5/FLOAT(NL)
                  DO 60 I=1,NL
145               II=I+K-1
                  SUM=SUM+ABS(S(I)-AB(II,J)+SUM5)
                  SUM2=SUM2+(S(I)-AB(II,J)+SUM5)**2
                60 CONTINUE
                  IF(SUM.GE.SUMR)GO TO 61
150               SUMR=SUM
                  KIR=K
                  KJR=J
                61 IF(SUM2.GE.SUMR2)GO TO 62
                  SUMR2=SUM2
155               KIR2=K
                  KJR2=J
                62 CONTINUE
                  ADIST=SQRT((FLOAT(KI1-KIR))**2+(FLOAT(KJ1-KJR))**2)
                  SDIST=SQRT((FLOAT(KI1-KIR2))**2+(FLOAT(KJ1-KJR2))**2)
160               PRINT 100,ADIST,SDIST
                  AD1=ADIST+AD1
                  SD1=SDIST+SD1
                  AD2=ADIST**2+AD2
                  SD2=SDIST**2+SD2
165              70 CONTINUE
                  AD1=AD1/10.
                  SD1=SD1/10.
                  AD2=AD2/10.
                  SD2=SD2/10.
170               PRINT 120,AD1,AD2,SD1,SD2
                72 CONTINUE
```

```
      REWIND 1
      PRINT 103,RA
      PRINT 112,RO
175   PRINT 114,NL
      CALL RANGET(DD)
       PRINT 107,DD
      STOP
  100 FORMAT(16X,F6.2,27X,F6.2)
180   101 FORMAT(13X,*MAD ERROR*,24X,*MSD ERROR*)
  102 FORMAT(1X,*PHI=*,F4.1)
  103 FORMAT(1X,*SIGMA T / SIGMA N =*,F4.1)
  104 FORMAT(1X,*NCTR=*,I3)
  105 FORMAT(1X,*CORRECT I.D.AT*,2I3,10X,2I3,1X,*MISTAKEN FOR*,2I3)
185   106 FORMAT(1X,*CORRECT I.D.AT*,2I3,10X,*CORRECT I.D.AT*,2I3)
  107 FORMAT(1X,*RANDOM NUMBER=*,E15.7)
  108 FORMAT(1X,2I3,1X,*MISTAKEN FOR*,2I3,5X,*CORRECT I.D.AT*,2I3)
  109 FORMAT(1X,2I3,1X,*MISTAKEN FOR*,2I3,5X,2I3,1X,*MISTAKEN FOR*,2I3)
  110 FORMAT(7X,*MAD*,32X,*MSD*)
190   111 FORMAT(1X,*AVE. MAD ERROR=*,1X,F5.1,11X,*AVE. MSD ERROR=*,1X,F5.1)
  112 FORMAT(1X,*RO=*,F5.2)
  113 FORMAT(60X,*NOISE SIGMA=*,E15.7,1X,*SIGNAL SIGMA=*,E15.7,
     1*S/N=*,F5.2)
  114 FORMAT(1X,*TRACK LENGTH =*,I3)
195   120 FORMAT(1X,*AD1=*,E10.4,1X,*AD2=*,E10.4,10X,*SD1=*,E10.4,1X,*SD2=*,
     1E10.4)
      END
```

```
      SUBROUTINE RAND2(RN1,RN2,SIGNO,FMEAN,ID)
      X=RANF(DUM)
      Y=RANF(DUM)
      IF(ID.EQ.1)GO TO 5
    5 RN1=X
      RN2=Y
      GO TO 10
    5 CC=SQRT(-2.*ALOG(X))*SIGNO
      RN1=CC*COS(6.28313*Y)+FMEAN
   10 RN2=CC*SIN(6.28313*Y)+FMEAN
   10 RETURN
      END
```

REFERENCES

1. Cannon, M.W. and J.W. Carl, June 1974, *TERCOM Performance: Analysis and Simulation*, AMRL-TR-73-130 (AD 783 804), Aerospace Medical Research Laboratory, Wright-Patterson Air Force Base, Ohio.

2. Summers, T.W., 1972, *TERCOM False Fix Study*, ASD-TR-72-74, Vol 4, Aeronautical Systems Division, Wright-Patterson Air Force Base, Ohio.

3. Moshman, J., 1960, "Random Number Generation," *Mathematical Methods for Digital Computers*, Ralston & Wilf, eds., New York: Wiley.

*U.S.Government Printing Office: 1978 — 757-080/682